Isı Bilimi ve Tekniği Dergisi, 43, 2, 191-205, 2023
J. of Thermal Science and Technology
©2023 TIBTD Printed in Turkey
ISSN 1300-3615
e-ISSN 2667-7725
https://doi.org/10.47480/isibted.1391419

TRNSYS MODEL OF THE COMBI BOILER DOMESTIC HOT WATER CIRCUIT WITH A FOCUS ON THE PARAMETER DEFINITION OF THE PLATE HEAT EXCHANGER

Okan Gök*, Ayşe Uğurcan Atmaca, Aytunç Erek*, and Hürrem Murat Altay*****
* Mechanical Engineering Department, Faculty of Engineering, Dokuz Eylül University Tınaztepe Yerleşkesi 35390 Buca, İzmir, Türkiye, gok.okan@ogr.deu.edu.tr; aytunc.erek@deu.edu.tr
** Aerospace Engineering Department, Faculty of Engineering, Dokuz Eylül University Tınaztepe Yerleşkesi 35390 Buca, İzmir, Türkiye, ugurcan.atmaca@deu.edu.tr
*** Bosch Termoteknik Isıtma ve Klima Sanayi Ticaret Anonim Şirketi, 45030 Manisa, Türkiye, murat.altay@tr.bosch.com

(Geliş Tarihi: 28.12.2022, Kabul Tarihi: 29.09.2023)

Abstract: Combi boilers used for both space and domestic hot water heating are one of the common household appliances. Modelling the domestic hot water circuit of a combi boiler for the preliminary evaluation of the laboratory testing is of crucial importance since it decreases the time, cost, and energy spent on the trials. There are various modelling approaches established by the authors of this paper. Domestic hot water circuit of the appliance is modelled previously making use of the Transient System Simulation Tool (TRNSYS 18) and a good agreement is achieved with the experimental and numerical data for the economic mode simulations. The drawback of the current TRNSYS model is the dependence on the experimental data for some of the parameter definitions of the components selected from the TRNSYS library, i.e. UA (multiplication of the overall heat transfer coefficient and the heat transfer area) input of the plate heat exchanger and heat retention effect of the heat cell block. In this paper, a constant value is assigned to the parameter definition of UA instead of a time dependent varied profile. Mean absolute errors covering the steady-state and transient operating regions for the domestic hot water inlet and outlet temperature difference in economic mode simulations stay nearly the same around 0,46°C, 0,82°C, and 0,53°C for 5 l/min, 7 l/min, and 8,7 l/min, respectively, under constant and variable UA approaches. Comfort operating scheme model is established with a couple of experimental data as of the principal application of the constant UA approach. Mean absolute error of the overall domestic hot water inlet and outlet temperature difference profile decreases to 0,5°C in the comfort mode simulation.
Keywords: Combi boiler, Transient system simulation, Plate heat exchanger (PHE), Domestic hot water (DHW), Comfort and economic (eco) operating modes, TRNSYS model, UA input.

PLAKALI ISI EŞANJÖRÜNÜN PARAMETRE TANIMI ODAKLI KOMBİ SICAK KULLANIM SUYU HATTININ TRNSYS MODELİ

Özet: Mahal ve sıcak kullanım suyu ısıtılması için kullanılan kombiler, yaygın olarak kullanılan ev aletlerindendir. Laboratuvar testlerinin ön değerlendirmesi için bir kombinin sıcak kullanım suyu devresinin modellenmesi, deneyler için harcanan zamanı, maliyeti ve enerjiyi azalttığı için oldukça önemlidir. Bu makalenin yazarları tarafından oluşturulan çeşitli modelleme yaklaşımları bulunmaktadır. Önceki çalışmalarda, cihazın sıcak kullanım suyu devresi *Zamana Bağlı Sistem Simülasyon Aracı* (TRNSYS 18) kullanılarak modellenmiştir ve ekonomik mod simülasyonları için deneysel ve sayısal veriler kullanılarak iyi bir uyum ortaya konmuştur. Mevcut TRNSYS modelinin dezavantajı, TRNSYS model kütüphanesinden seçilen bileşenlerin, plakalı ısı eşanjörünün UA (toplam ısı transfer katsayısı ve ısı transfer alanının çarpımı) girdisi ve ısı hücresi bloğunun ısı tutma etkisi gibi bazı parametre tanımlarının deneysel verilere bağımlı olmasıdır. Bu makalede, plakalı ısı eşanjörünün UA parametresi zamana bağlı değişken bir profil yerine sabit bir değer olarak tanımlanmıştır. Kombinin ekonomik çalışma modu simülasyonlarında, sıcak kullanım suyunun giriş ve çıkış sıcaklık farkı için kararlı ve kararsız süreçleri kapsayan ortalama mutlak hatalar, sabit ve değişken UA yaklaşımları altında 5 l/dk, 7 l/dk ve 8.7 l/dk için sırasıyla 0.46°C, 0.82°C ve 0.53°C olarak neredeyse sabit kalmıştır. Konfor çalışma modunun modeli, sabit UA yaklaşımının önemli bir uygulaması olarak birkaç deneysel veri ile oluşturulmuştur. Konfor modu simülasyonunda, sıcak kullanım suyu giriş ve çıkış sıcaklık farkı profilinin ortalama mutlak hatası 0.5°C'ye düşmektedir.
Anahtar Kelimeler: Kombi, Zamana bağlı sistem simülasyonu, Plakalı ısı değiştiricisi (PID), Sıcak kullanım suyu (SKS), Konfor ve ekonomik (eco) çalışma modları, TRNSYS modeli, UA girdisi.

INTRODUCTION

Combi boilers are one of the mostly used appliance groups for the residence since they are used for both space and domestic hot water (DHW) heating functions. Combi boilers are simple devices since they include a primary heat exchanger, a secondary heat exchanger, a pump, and a diverter valve as given in Figure 1. Primary heat exchanger is the heat cell (HC) including the combustion of the natural gas at which the energy of the hot combustion products is transferred to the central heating (CH) water. The CH water is sent to the radiators to warm up the surroundings when the space heating function is active. The space and DHW heating function cannot be activated at the same time, hence when the user DHW demand is created, space heating function stops. At the time of the user DHW demand, the diverter valve changes the direction of the flow and the CH water is sent through the secondary heat exchanger named as plate heat exchanger (PHE). Therefore, DHW is provided users after the energy of the hot CH water is transferred to the DCW in the PHE.

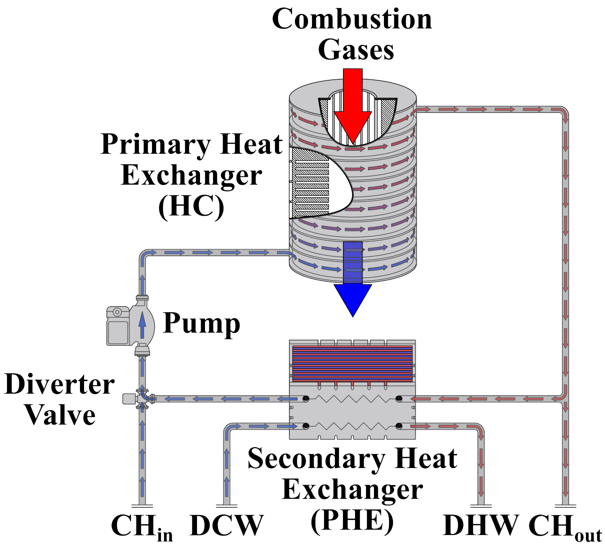

Figure 1. Schematic view of the combi boiler heater with the basic equipment

The subject of this paper is modelling the DHW heating circuit of the combi boiler type heating appliances. This study is a continuation of the previous studies established by the authors of these studies. First of the milestone studies of the research group is the one-dimensional (1D) model of the DHW heating circuit (Atmaca et al., 2015). 1D transient heat transfer equations were solved simultaneously to calculate the temperature profiles of the CH water at the inlet and outlet of the HC and the temperature difference of the DHW between the PHE inlet and outlet and the agreement was found satisfactory at various operating conditions especially for the steady-state region. Secondly, a commercial 1D thermal-fluid system modelling software, Flowmaster® was used to create the model of the DHW function of the combi boiler (Atmaca et al., 2016). CH inlet and outlet temperatures from the HC resulted in approximately 10 K higher values than the experimental data even in the steady-state region. Since the heat transfer rates and the DHW temperature difference between the inlet and outlet of the PHE were compared in main, the Flowmaster® model as well was found appropriate to be used in the preliminary evaluations. The essential drawback with this model was the parameter definition concerned with the HC, i.e. implementation of the heat retention effects of the HC. Lastly, DHW heating circuit was modelled using the Transient System Simulation Tool (TRNSYS 18) (Klein et al., 2017) and the model achieved a good agreement with the experimental data for both the steady-state and transient temperature profiles of the economic (eco) mode simulations at various operation conditions (Gök et al., 2022). Subsequently, both experimental and numerical validations were displayed elaborately for the CH inlet and outlet temperatures from the HC and the DHW inlet and outlet temperature difference from the PHE at 5 l/min, 7 l/min, and 8,7 l/min DHW user demands in economic mode simulations (Gök et al., 2023). However, the TRNSYS model needed improvement since it was highly dependent on the experimental data.

When compared to the previous studies of the authors regarding the use of TRNSYS, this current research has two main objectives as to decrease the dependence of the TRNSYS model on the experimental data and to define appropriate parameter definition of the model for the comfort mode validation. The TRNSYS model needs experimental data for the UA parameter definition of the plate heat exchanger and the heat retention effect of the HC block. In the firstly established TRNSYS models (Gök et al., 2022 and Gök et al., 2023), UA profile of the PHE was inserted into the model with respect to the transient behavior of the appliance. When compared to the previous 1D DHW circuit model, the temperature profiles of the CH water and DHW were estimated with less mean absolute errors (MAE), mean square errors (MSE), and root mean square errors (RMSE) for the overall time duration including the transient and steady-state regions. Besides, in this study, the effects of the insertion of the transient UA profile and an average UA value into the model on the MAE, MSE, and RMSE are compared and the influence of this UA parameter definition is discussed in detail. Moreover, comfort mode validation is made with regard to this crucial finding.

Part of the literature studies conducted by the authors of this paper is summarized in the aforementioned paragraphs in order to highlight the objectives of the paper clearly. There are various studies as well in the literature concerning DHW heating, combi boilers, and TRNSYS models of the systems other than the formerly summarized studies of the authors. Five different domestic hot water heater concepts were investigated by Boait et al. (2012) and they highlighted the higher efficiency of the instantaneous hot water systems when compared to the systems with storage tanks. Moreover, the authors also discussed the temperature ranges of DHW to prevent scalding and to mitigate the risk of Legionella in the system. Pärisch et al. (2019) investigated tankless water heaters (instantaneous water heaters) using hot water as the energy source. The authors of this paper as well gave the critical temperature limits with respect to typical system characteristics, i.e. exchange frequency of water within the system, the volume of the water between the heater and each tap, etc. They focused on the comfort properties of DHW under transient conditions rather than other challenging design parameters of capacity and energy efficiency. A new test procedure proposal for comfort evaluations was given with future work discussion. Pomianowski et al. (2020) prepared a review paper on the recent developments covering the production, storage, circulation, and distribution of DHW from the viewpoints of energy use and efficiency. They pointed out the attitude of the latest studies focusing on the DHW production. Haissig and Woessner (2000) explained the adaptive fuzzy control (AFC) algorithm in detail. In comparison with a traditional proportional-integral-derivative (PID) controller which was commonly used in combi-boilers, set-point error and control effort were reduced between 18%-70% and 23%-41%, respectively due to the development of AFC. Lastly, there are review studies covering DHW heating systems with various perspectives. İbrahim et al. (2014) presented a literature review of the DHW production systems categorizing them into six groups as wood, oil/gas, electric, heat pump, solar and instantaneous systems.

As of the previous studies concerned with the combi boilers, there are many other researches in addition to previously given studies (Atmaca et al., 2015; Atmaca et al., 2016; Gök et al., 2022; and Gök et al., 2023). Ucar and Arslan (2021) stated that the combustion unit including the main heat exchanger had the highest contribution to the total exergy destruction with reference to the advanced exergy analysis for the space heating function of 24 kW commercial condensed combi boiler. Hence space heating efficiency could be improved to 14.32% due to the improvements made on the combustion process and main heat exchanger. Fridlyand et al. (2021) used EnergyPlus to establish a simple simulation tool to calculate the energy consumption of the tankless combi boilers since EnergyPlus is a widely used and open source energy simulation program. The proposed Lumped Heat Capacity combi model could be used to compare the effects of the various control strategies and to evaluate the amount of the energy savings of the modern combi concepts when compared to the regular/traditional appliances. Quintã et al. (2019) constructed the mathematical model of the tankless gas water heaters via lumped space approach. There were challenging targets concerned with the efficiency, comfort, and emissions of the flue gas. Therefore, the proposed model was useful to test /simulate various appliance concepts and control algorithms in order to optimize the efficiency, the comfort level of the users, and the emissions of the harmful gases.

In the last part of the literature survey, TRNSYS models are summarized. In the study of Jordan and Vajen (2001), four categories were specified to generate different types of loads. Effects of the DHW flow rate and the draw-off time of the day under realistic and simplified DHW profiles with respect to two different designs of the discharge unit on the fractional energy savings were analyzed. Andrés and López (2002) constructed a new physical model of a solar domestic water heater with a horizontal storage and mantle heat exchanger making use of TRNSYS. The main distinction of their model was the place of the hot fluid inlet at the upper of the mantle heat exchanger annulus. The comparison for the delivered daily energy between the model results and the experimental data yielded error less than 3%. Nordlander and Persson (2003) built the first simulation study of the pellet stoves to be used in house heating with TRNSYS using the type 140 and type 210 in order to model the convection and storage mechanism with the combustion phenomenon. Experimental measurements were used for the model specification in order to determine some of the component parameters and the validation. Persson et al. (2009) created the dynamic model of small pellet boilers and stoves for house heating via TRNSYS. The methodology of the paper was comprised of laboratory measurements of boilers and stoves, modelling and parameter definition, and model validation. Although the agreement between the model results and measurements was found generally satisfactory, improvements were required for large water volumes. Bourke and Bansal (2012) expressed the thermal efficiency of the gas instantaneous water heater with respect to the operating conditions by an equation in order to be used in the TRNSYS model to include the efficiency variations of this water heater and to yield more accurate energy consumption calculations. Persson et al. (2019) established a boiler model combining two of the existing models in TRNSYS as Type 210 and Type 341 which is a modified version of Type 340. The pellet burner was modelled using the Type 210. The flue gas heat exchanger and boiler water volume were established under Type 341. They could model the thermal behavior of the boilers, namely stratification and the thermal response, more accurately with respect to previously established models. Braas et al. (2020) used TRNSYS in their study to model four sub-station types including two instantaneous and two storage systems for the single family and multifamily houses in order to establish realistic DHW load profiles. Harrabi et al. (2021) analyzed the performance of the solar collector for DHW production with the help of TRNSYS. An additional storage tank as well was considered with the tank of the collector.

There are various TRNSYS modelling studies regarding the space and DHW heating (Antoniadis and Martinopoulos, 2019; Villa-Arrieta and Sumper, 2018; and Lu et al., 2021). All these exemplified studies highlight that TRNSYS is an effective and valuable tool for the transient system modelling. Moreover, Shrivastava et al. (2017) presented a literature review regarding the solar water heaters with respect to the system analyses simulations and they focused on the TRNSYS software throughout the paper due to the wide use of the program in the simulations. They also showed the necessity of the simulations since they decrease the testing time and cost with the preliminary evaluations, simplify the complicated phenomenon, and enable efficient source utilization. Hence the outstanding motivation of this study is the importance of the construction and development of the combi boiler DHW circuits for the preliminary system evaluations to decrease the number of test trials and improving the reliance of the simulation model on the experimental data to analyze the system performance for a wide range of operating conditions.

For the variable and constant UA comparisons, the temperature profiles of CH water inlet and outlet from the HC and DHW inlet and outlet temperature difference of the PHE calculated making use of TRNSYS model are declared with the experimental data. Mean absolute error (MAE), mean square error (MSE), and root mean square error (RMSE) are tabulated for both UA insertion approaches. Moreover, for the comfort mode validation after showing the applicability of the constant UA approach, the DHW inlet and outlet temperature difference of the PHE from TRNSYS model is compared with the results calculated by the previously established 1D model (Atmaca et al., 2015) with respect to the experimental data. The same regression metrics for the comfort mode simulation of the TRNSYS model and 1D model are presented. As a result, comfort mode validation according to the constant UA approach yields a more satisfactory agreement with the experimental data for the transient region than the 1D model.

OPERATIONAL SCHEMES OF A COMBI BOILER

Two operating modes are examined in this study as economic (eco) and comfort modes for the DHW heating function. The distinction between these two operating modes is apparent from the temperature profile comparisons of DHW at the PHE outlet as given in Figure 2. In the eco mode, when the users request DHW, the appliance starts ignition and there is a transient region in the temperature profile of the DHW outlet since all of the system components are at the ambient temperature and store some of the released energy until the system reaches the steady-state operating condition.

In the comfort mode, hot CH water is kept within the system to decrease the transient region in the DHW outlet temperature and hence the user comfort is improved. According to the operation algorithm of the appliance, the CH water in the HC is heated regularly until its temperature reaches an upper set point, i.e. 60°C, whenever the temperature decreases below another lower set point as exemplified in Figure 3. The appliance keeps hot CH water within the system to provide the DHW directly for the higher comfort level of the users although keeping hot CH water all the time within a temperature range is disadvantageous in terms of efficiency.

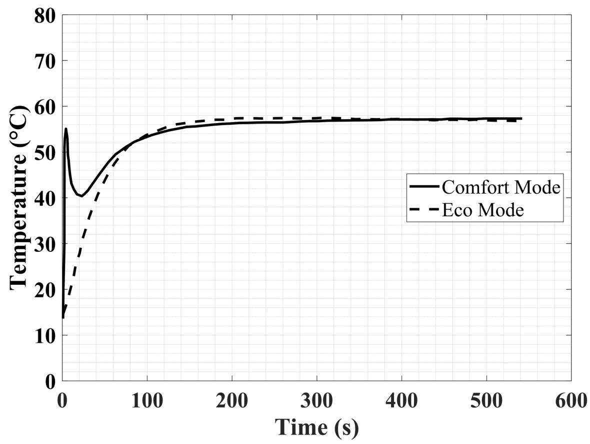

Figure 2. Comparison of the DHW outlet temperature profile between the eco and comfort operating schemes (Atmaca et al., 2015).

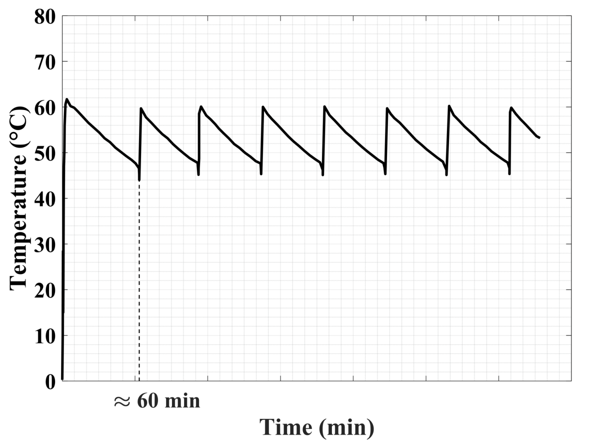

Figure 3. Variation of the CH water temperature throughout the preheat cycles in the comfort mode (Atmaca et al., 2015).

MODELLING APPROACHES

Main model of this study is established with the help of TRNSYS. Variable and constant UA approaches are compared according to the results obtained from this model. However, for the comfort operating mode validations, the results obtained from previously established 1D model as well are used to show the superiority of the TRNSYS model. Hence, 1D HC and PHE modelling equations are introduced briefly with reference to Atmaca et al. (2015).

1D Model Governing Differential Equations

1D model of the DHW circuit is constructed with five equations, namely the flue gas cooling, the CH water heating in the HC, the HC wall heating, the CH water cooling in the PHE, and the DHW heating. Differential control volumes of the HC and the PHE on which the governing equations are derived are given in Figure 4 (a) and (b), respectively, as well as the flow directions of each fluid domain. The details concerned with the solution algorithm of these five equations are described by Atmaca et al. (2015).

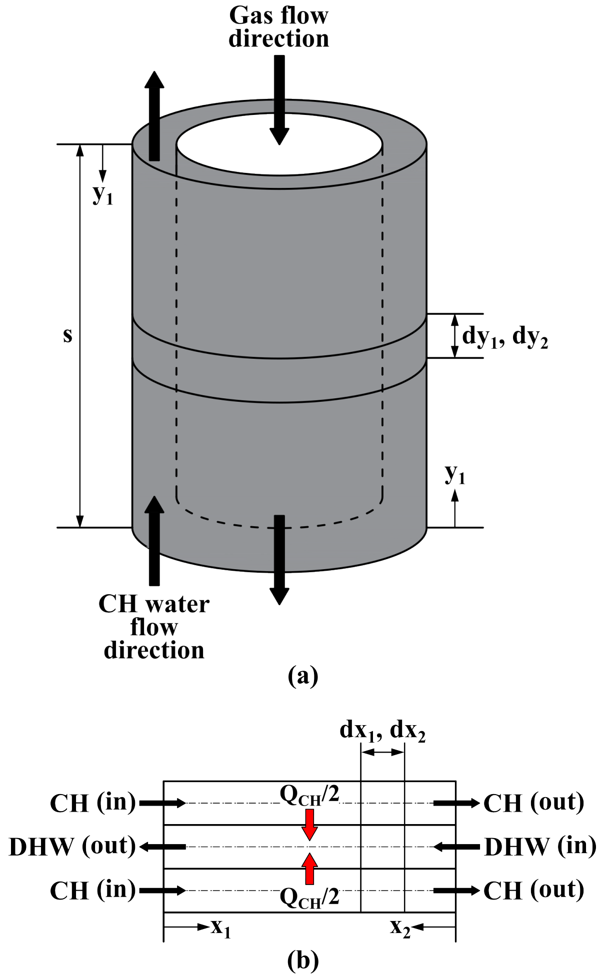

Figure 4. Differential control volumes on which the governing equations are derived and the flow directions of (a) the HC and (b) the PHE (Atmaca et al., 2015).

The first three equations belong to the HC and describe the cooling of the flue gas, the heating of the CH water in the HC, and the heating of the HC wall. The total thermal resistances between the HC wall and the flue gas, and the HC wall and the CH water are determined theoretically. The fourth equation shows the cooling of the CH water and the fifth equation declares the heating of the DHW in the PHE. The multiplication of the overall heat transfer coefficient and the heat transfer area (UA) for the PHE is determined experimentally to be used in the numerical calculations. The terms on the left side of the equation shows the rate of change of thermal energy stored within the control volumes. Hence, due to these terms, the variation of the temperature from the transient regions to steady-state regions could be calculated.

$$\rho_g A_{c,g} c_{p,g} \frac{\partial T_g}{\partial t} = -\dot{m}_g c_{p,g} \frac{\partial T_g}{\partial y_1} - \frac{A_{s,g} U_g}{s} (T_g - T_w) \quad (1)$$

$$\rho_{wt} A_{c,wt(1)} c_{p,wt} \frac{\partial T_{wt(1)}}{\partial t} = -\dot{m}_{wt(1)} c_{p,wt} \frac{\partial T_{wt(1)}}{\partial y_2} + \frac{U_{wt(1)} A_{s,wt(1)}}{z} (T_w - T_{wt(1)}) - h_\infty \frac{A_o}{z} (T_{wt(1)} - T_\infty) \quad (2)$$

$$\rho_w A_{c,w} c_w \frac{\partial T_w}{\partial t} = k_w \frac{\partial^2 T_w}{\partial y_2^2} A_{c,w} + \frac{U_g A_{s,g}}{s} (T_g - T_w) - \frac{U_{wt(1)} A_{s,wt(1)}}{s} (T_w - T_{wt(1)}) \quad (3)$$

$$\rho_{wt} \frac{V_{chwc}}{l_{PHE}} c_{p,wt} \frac{\partial T_{wt(2)}}{\partial t} = -\dot{m}_{wt(2)} c_{p,wt} \frac{\partial T_{wt(2)}}{\partial x_1} - 2 \frac{U_{PHE} A_{PHE}}{l_{PHE}} (T_{wt(2)} - T_{wt(3)}) \quad (4)$$

$$\rho_{wt} \frac{V_{dhwc}}{l_{PHE}} c_{p,wt} \frac{\partial T_{wt(3)}}{\partial t} = -\dot{m}_{wt(3)} c_{p,wt} \frac{\partial T_{wt(3)}}{\partial x_2} + 2 \frac{U_{PHE} A_{PHE}}{l_{PHE}} (T_{wt(2)} - T_{wt(3)}) \quad (5)$$

The boundary condition of the flue gas equation is the adiabatic flame temperature as follows;

$$T_g(0,t) = T_{adia} \quad (6)$$

The boundary condition of the second and fourth equations are interconnected to each other since the CH water entering the HC is the CH water leaving the PHE and the CH water at the inlet of the PHE comes from the HC outlet as formulated below;

$$T_{wt(1)}(0,t) = T_{wt(2)}((l_{PHE}/dx_1), t) \quad (7)$$

$$T_{wt(2)}(0,t) = T_{wt(1)}((z/dy_2), t) \quad (8)$$

The wall heating equation includes the heat transfer term by conduction resulting in second order differential equation. Therefore, two boundary conditions are given as the convection surface condition (Incropera et al., 2007) and expressed by

$$\left(-k_w \frac{\partial T_w}{\partial y_2}\right)_{y_2=0} = h_\infty \left(T_\infty - T_w(0,t)\right) \quad (9)$$

$$\left(-k_w \frac{\partial T_w}{\partial y_2}\right)_{y_2=s/dy_1} = h_\infty (T_\infty - T_w((s/\, dy_1), t)) \quad (10)$$

The boundary condition of the DHW heating equation in the HC comes from the test conditions given as

$$T_{wt(3)}(0,t) = 10°C \quad (11)$$

The initial conditions for all of the equations are the same as the test conditions as

$$T_{g,wt(1),w}(y_{1,2}, 0) = 10°C \quad (12)$$

$$T_{wt(2),wt(3)}(x_{1,2}, 0) = 10°C \quad (13)$$

TRNSYS Model

TRNSYS v18 (Transient System Simulation Tool) is a dynamic simulation software consisting of different modules for modelling various electrical and thermal systems such as heating/cooling, HVAC, and alternative energy sources etc., developed by a group of academicians at the University of Wisconsin, USA (Klein et al., 2017). TRNSYS v18 is composed of two parts. The first part named as the kernel reads and processes the inputs defined by the user or the selected model, iteratively solves the system/model equations, determines the convergence, and creates the system variables. The name of the second part is the user interface that contains the models of the system components called "Type" in its existing libraries.

In this study, the TRNSYS model as shown in Figure 5 is created by selecting the types in the TRNSYS library according to the characteristics of each combi-boiler component in order to simulate the DHW circuit of the combi-boiler. The black, red, and blue line indications given in Figure 5 represent the three main subsections of the TRNSYS model, namely the component adjustment and the controlling tools, the CH water flow circuit, and the DHW flow circuit, respectively. Unlike the designation of the lines in Figure 5, in the schematic display of the combi-boiler DHW circuit in Figure 1, red and blue arrows represent the hot and relatively cold water of the CH water and DHW, respectively.

created as the output of this module. The variation of the HC load, i.e. heat retention effect of the heat cell block in the CH water circuit, and the power modulation are obtained from the Type 62 - Calling External Programs: Excel™ module by using the simulation time and nominal power values provided by the Equa module. Nominal power values for DHW flow rates of 5 l/min, 7 l/min and 8.7 l/min are presented as Equa module outputs. Besides, they are the inputs of the Type 62 module as given in Table 1. The time-dependent percentage power modulation values are presented in the plots of the Result and Discussion section for each DHW flow rate. Using the power modulation variations and the nominal power values, the amount of energy obtained from the combustion gases in the heat cell of the combi boiler is calculated through the following equation

$$\dot{Q}_{comb,in} = P\varphi \tag{14}$$

In the previously established TRNSYS model (Gök et al., 2022 and Gök et al., 2023), the multiplication of the overall heat transfer coefficient and the heat transfer area (symbolized by the UA designation) of the PHE as well is the output provided by the Type 62 - Calling External Programs: Excel™ module. The required measurements in order to define the time-dependent power modulation,

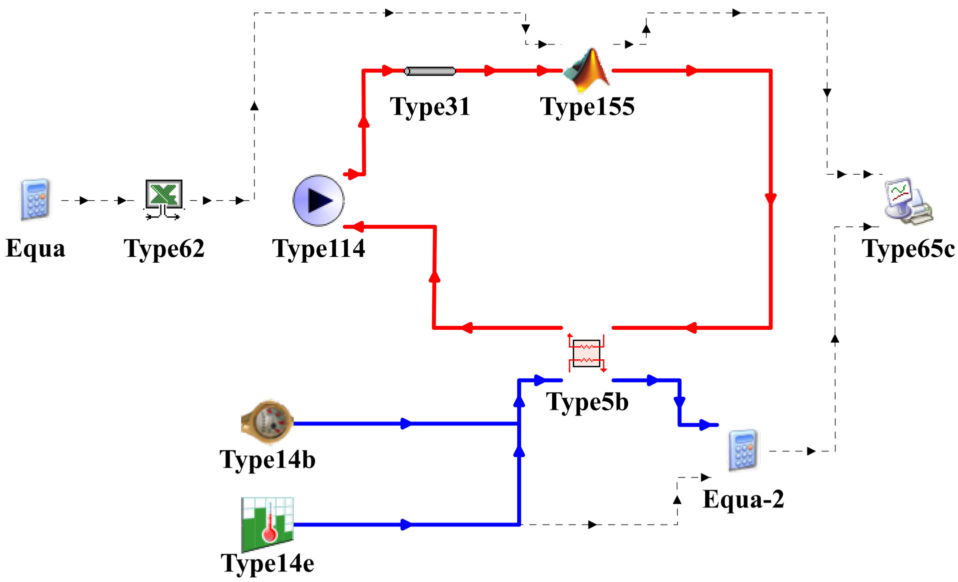

Figure 5. Flow diagram created in the TRNSYS interface for the DHW circuit model of the combi boiler.

These subsections are used to define the DHW circuit, CH water loop, and the inputs/outputs specifications for the control and connection of the model components. Therefore, the components of the DHW heating function simulation model selected from the TRNSYS existing library are presented in Table 1 with this extent covering their parameters, inputs, and outputs. The first subsection of the DHW circuit model for the adjustment and control tools is indicated by the dashed black lines. When the components in the TRNSYS model presented in Figure 5 are evaluated in hierarchical flow order, the module providing the first input to the simulation is Equa. The simulation time value and the nominal power input of the combi boiler depending on the DHW user demand are

UA input, and the HC load profile are explained thoroughly in the Experimental Test Rig section. The variation of the UA input in the transient and steady-state operating regions is given in Figure 6 for various operating conditions of 5 l/min, 7 l/min, and 8,7 l/min DHW user demands. In this study, the results are calculated using constant UA inputs and the comparison between the constant and variable UA input approaches is one of the main outcomes.

In Figure 6, there are two UA input variation lines for the 8,7 l/min DHW flow rate as the eco and comfort modes. Eco mode variations of the UA input are derived directly from the experimental data as used in the previous

TRNSYS model (Gök et al., 2022 and Gök et al., 2023). However, the UA input variation for the comfort mode is estimated under constant UA approach which is described in the subsequent regarding section. Therefore, in the previous TRNSYS model, UA input definition is made using the output of Type 62 and then becomes the input of Type 5b – Counterflow Heat Exchanger, whereas in the current TRNSYS model, the constant UA is directly defined as the input of Type 5b.

The last components of first main subsection indicated by the dashed black line are Equa-2 and Type 65c - Online Plotter. Using the Type 65c, the calculated temperature difference of the DCW and DHW, the CH water inlet temperature, and the CH water outlet temperature from the HC are printed. The temperature difference between the DHW and the DCW of the PHE is calculated in Equa-2 module as follows

$$\Delta T_{DHW} = T_{DHW} - T_{DCW} \tag{15}$$

The second subsection displayed by the red lines is the CH water flow circuit in which the combustion of the natural gas is replaced by the heat input definition. The selected components from the TRNSYS existing library given in the red circuit are Type 114 - single speed pump model providing fluid drive and used to define the CH water mass flow rate, Type 31 - pipe model representing the piping in the CH water circuit, Type 5b - counterflow heat exchanger model (representing the plate heat exchanger) in which the heat is transferred from the CH water circuit to the DHW circuit, and Type 155 - MATLAB model for the heat cell component where heat input is defined simply instead of the natural gases combustion. Moreover, the heat retention effects of the heat cell block are calculated in Type 155. In line with the difference between the heat input provided by the natural gas combustion and the heat retention of the heat cell which is defined as the HC load, the amount of the energy transferred to the CH water and the temperature of the CH water at the HC outlet are calculated in Type 155 as

$$\dot{Q}_{CH,net} = \dot{Q}_{comb,in} - \dot{Q}_{HC,load} \tag{16}$$

$$T_{CH,HC,out} = T_{CH,HC,in} + \frac{\dot{Q}_{CH,net}}{(\dot{m}_{CH} c_{p,wt})} \tag{17}$$

Time dependent data of the heat retention effects for the HC transferred from the Type 62 outputs is the input of Type 155. Implementation of the heat retention effects is of crucial importance for the transient temperature profile of the DHW and the CH water. The time-dependent heat cell load profiles for the various DHW user demands are given in Figure 7. The main reason for this time-dependent load profile definition requirement is the lack of mass content to store heat in the components used for the simulations in TRNSYS software. In Figure 7, the load is calculated as minus at some regions due to the instantaneous power modulation of the appliance. There are two load profiles for 8,7 l/min DHW flow rate for the eco and comfort modes both of which are explained in the regarding subsequent section.

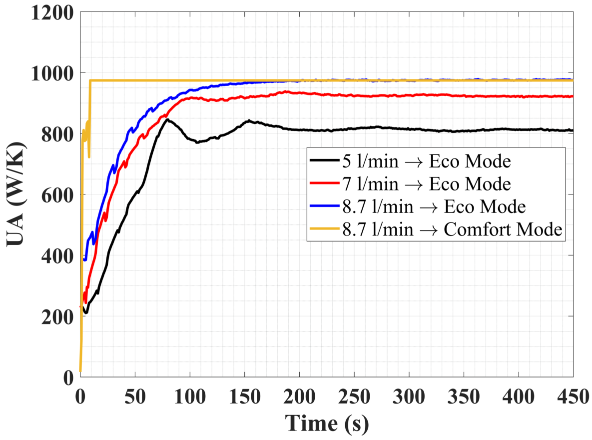

Figure 6. Variation of the UA input for the Type 5b - Counterflow Heat Exchanger module

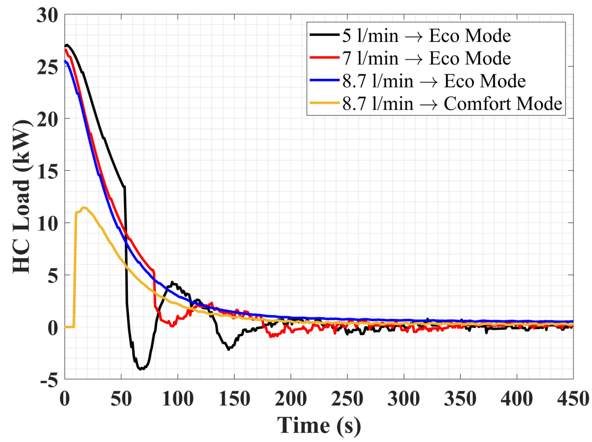

Figure 7. Time-dependent variation of the load profile for representing the heat retention effects of the heat cell

The third main sub-section designated by the blue lines is for obtaining the DHW by heating the DCW according to the user demand. In the blue circuit, Type 14b and Type 14e modules are time dependent forcing functions and used for mass flow rate specification and temperature declaration components, respectively. The provided time-dependent data from Type 14b and Type 14e outputs are transferred to Type 5b. Furthermore, the blue circuit passes on the load side of Type 5b and the red circuit passes on the source side of this module. All aforecited modelling details are summarized in Table 1.

EXPERIMENTAL TEST RIG

Experimental measurements are collected from the test rig given in Figure 8. CH inlet and outlet temperatures from the HC and DHW inlet and outlet temperatures from the PHE are measured for the experimental verification. Moreover, these temperature measurements are not only used in the validations, but for the parameter definition of some of the components as well in the TRNSYS model.

Table 1. Summary of the Type selection and definition of the DHW circuit model in TRNSYS

Type Name	Parameters		Inputs		Outputs	
Equa	–		–		Time (s)	Simulation Time
					P (kW)	17.6 24.6 27.5
Type 62	–		Time (s)	Simulation Time	$\dot{Q}_{comb,in}$ (kW)	Time dependent
			P (kW)	17.6 24.6 27.5	$\dot{Q}_{HC,load}$ (kW)	Time dependent
Type 114	$\dot{m}_{rated}$ (kg/s)	0.3742	$\dot{m}_{CH,pump,in}$ (kg/s)	0.3742	$\dot{m}_{CH,pump,out}$ (kg/s)	0.3742
	$c_{p,water}$ (kJ/kg.K)	4.19	$T_{CH,pump,in}$ (°C)	Calculated Value	$T_{CH,pump,out}$ (°C)	Calculated Value
	P_{rated} (kW)	0.03				
Type 31	$D_{pipe,inner}$ (m)	0.0165	$\dot{m}_{CH,pipe,in}$ (kg/s)	0.3742	$\dot{m}_{CH,pipe,out}$ (kg/s)	0.3742
	L_{pipe} (m)	1				
	$\rho_{pipe,inner}$ (m)	1000	$T_{CH,pipe,in}$ (°C)	Calculated Value	$T_{CH,pipe,out}$ (°C)	Calculated Value
	$c_{p,water}$ (kJ/kg.K)	4.19				
	$T_{CH,pump,initial}$ (°C)	10				
Type 155	–		$\dot{m}_{CH,HC,in}$ (kg/s)	0.3742	$\dot{m}_{CH,HC,out}$ (kg/s)	0.3742
			$T_{CH,HC,in}$ (°C)	Calculated Value		
			$\dot{Q}_{comb,in}$ (kW)	Time dependent	$T_{CH,HC,out}$ (°C)	Calculated Value
			$\dot{Q}_{HC,load}$ (kW)	Time dependent		
Type 14b	$t_{initial}$ & t_{final} (s)	0…500	–		$\dot{V}_{DHW}$ (l/min)	5 7 8.7
	$\dot{V}_{DHW}$ (l/min)	5 7 8				
Type 14e	$t_{initial}$ & t_{final} (s)	0…500	–		T_{DCW} (°C)	10
	T_{DCW} (°C)	10				
Type 5b	–		$\dot{m}_{CH,PHE,in}$ (kg/s)	0.3742	$\dot{m}_{CH,PHE,out}$ (kg/s)	0.3742
			$T_{CH,PHE,in}$ (°C)	Calculated Value		
			$\dot{V}_{DHW}$ (l/min)	5 7 8.7	$T_{CH,PHE,out}$ (°C)	Calculated Value
			$T_{DHW,PHE,in}$ (°C)	10	$\dot{V}_{DHW}$ (l/min)	5 7 8.7
			UA (W/K)	812 923.9 974.7	T_{DHW} (°C)	Calculated Value
Equa-2	–		T_{DCW} (°C)	10	ΔT_{DHW} (°C)	Calculated Value
			T_{DHW} (°C)	Calculated Value		
Type 65c	–		$T_{CH,HC,in}$ (°C)	Calculated Value	–	
			$T_{CH,HC,out}$ (°C)	Calculated Value		
			ΔT_{DHW} (°C)	Calculated Value		

First of all, power profiles are recorded for all of the investigated DHW flow rates and they are inserted into 1D model and TRNSYS models including variable and constant UA approaches. Secondly, UA variation is calculated based on these abovementioned temperature measurements under the variable UA parameter approach. The amount of heat transferred to the DHW could be calculated from the adjusted DHW flow rate and the inlet and outlet temperature difference of DHW from the PHE. Since the inlet and outlet temperatures of the CH water and DHW from the PHE are measured, the logarithmic mean temperature difference could be calculated. Hence, the variation of UA is obtained. In 1D modelling approach, a separate test rig was used to define the UA of the PHE and an average UA value at the steady-state operating condition is used for each investigated case (Atmaca et al., 2015). Lastly, the load profile is defined similarly by subtracting the heat gain of the DHW from the measured power of the appliance. This difference is used to represent the stored energy by the HC block. Therefore, heat retention effect of the HC which is a key parameter in order to obtain the transient temperature profile of the CH water and DHW could be inserted into the model.

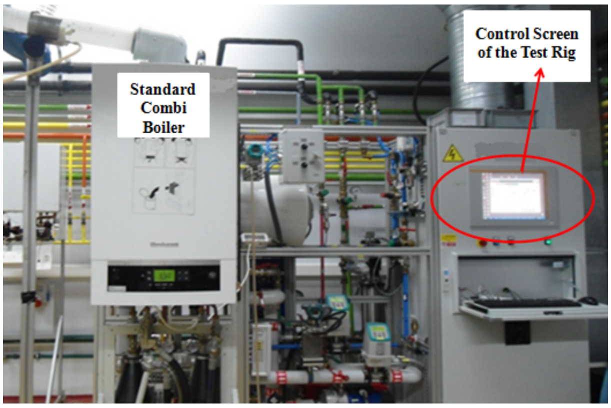

Figure 8. Combi boiler test rig for the temperature measurements of the CH water and DHW

RESULTS AND DISCUSSION

The preliminary results between the 1D modelling approach and the TRNSYS model yielded the superiority of the TRNSYS model over the 1D model with the decreased MAE, MSE, and RMSE for the overall temperature profile covering the transient region (Gök et al., 2022 and Gök et al., 2023). The most important disadvantage of the TRNSYS model is the use of the experimental UA variation and the load profile to represent the heat retention effects of the HC. First of all, UA variation is replaced with a constant UA value which is determined as the average of the UA values from the steady-state region in the TRNSYS model. The concluding remarks are interpreted with reference to some important regression metrics as mean absolute error (MAE) which is the average of the absolute errors between the estimated values and measured data, mean square error (MSE) defined as the average of the square of the errors, and root mean square error (RMSE) expressed as the square root of the MSE. They are all formulated as follows;

$$MAE = \frac{1}{n}\sum_{i=1}^{n}\left|y_{exp,i} - y_{theo,i}\right| \quad (18)$$

$$MSE = \frac{1}{n}\sum_{i=1}^{n}\left(y_{exp,i} - y_{theo,i}\right)^2 \quad (19)$$

$$RMSE = \sqrt{\frac{1}{n}\sum_{i=1}^{n}\left(y_{exp,i} - y_{theo,i}\right)^2} \quad (20)$$

Comparison of the Variable and Constant UA Approaches for the PHE

This section focuses only the parameter definition of the multiplication of the overall heat transfer coefficient and the heat transfer area, designated simply as UA, of the PHE in eco working mode. Figure 9 (a), (b), and (c) shows the comparison between the constant and variable UA approaches with respect to the experimental data for the CH water inlet temperature of the HC, CH water outlet temperature of the HC, and DHW inlet and outlet temperature difference of the PHE, respectively, at 5 l/min DHW user request. It is obvious that both approaches result in a good agreement with the experimental data.

At the DHW user request of 5 l/min, MAE of the steady state temperature profile is around 0.7 ˚C for CH water inlet temperature and approximately 0.4 ˚C for the CH water outlet temperature and DHW inlet and outlet temperature difference under both approaches. For the overall temperature profile of the same DHW flow rate including the transient region, constant UA approach results in slightly higher MAE of CH water inlet and outlet temperatures, but the maximum of these errors is 1.6 ˚C which is still acceptable for this kind of modelling tools and assumptions as tabulated in Table 2 and Table 3. However, as of the most critical performance indicator of the combi boiler DHW heating function, the MAE of the DHW inlet and outlet difference is about 0.5 ˚C for both of the approaches as displayed in Figure 9 (c) with the great consistency in the temperature variations.

Similarly, Figure 10 (a), (b), and (c) make comparison between these two approaches according to the experimental data at the 7 l/min DHW user demand for the CH water inlet temperature of the HC, CH water outlet temperature of the HC, and DHW inlet and outlet temperature difference. MAE values of the steady-state temperature profiles are around 0.5˚C, 1˚C, and 0.4˚C for the CH water inlet temperature, CH water outlet temperature, and DHW inlet and outlet temperature difference, respectively, under both approaches. For the overall temperature profiles of the same DHW flow rate, the MAE values calculated by constant UA approach either decrease or slightly increase when compared to the errors of the variable UA assumption.

User requests at the DHW flow rates of 5 l/min and 7 l/min result in power modulation according to the control algorithm of the appliance as plotted in the secondary axes of Figure 9 and Figure 10. However, the last comparison given in Figure 11 and made for the 8.7 l/min DHW user request does not include any power modulations. Figure 11 (a), (b), and (c) presents the comparative plots of the CH water inlet temperature of the HC, CH water outlet temperature of the HC, and DHW inlet and outlet temperature difference, respectively, for 8,7 l/min DHW flow rate.

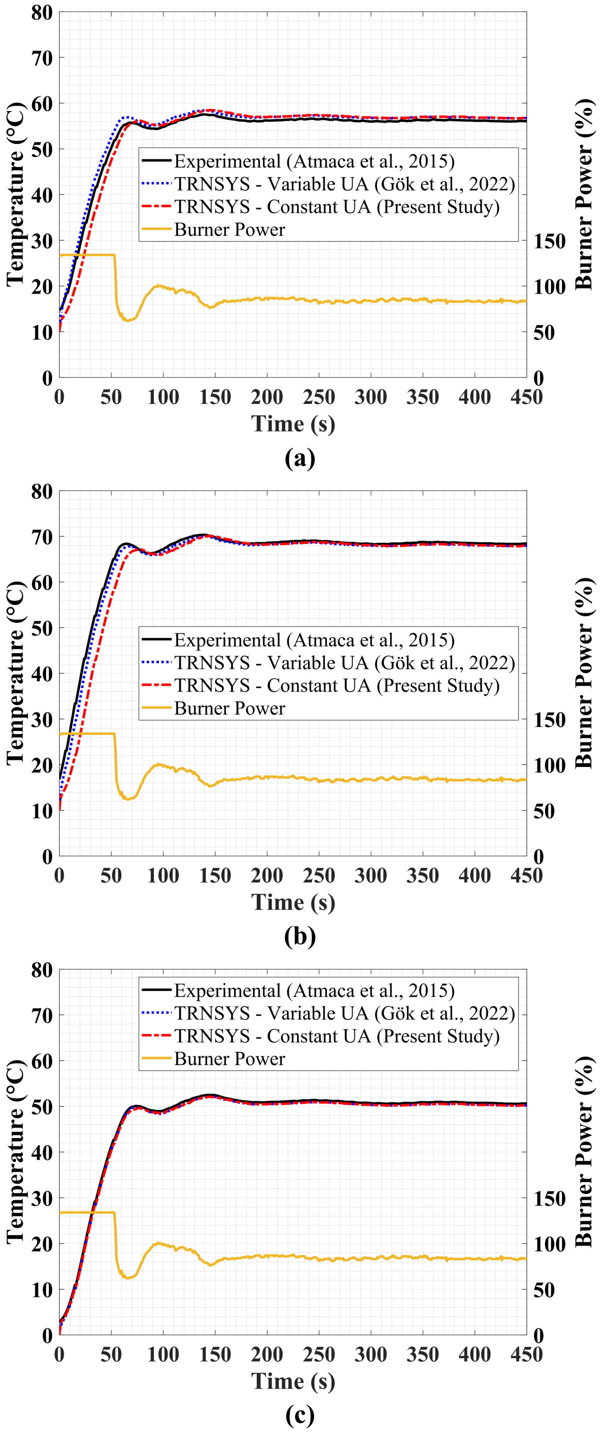

Figure 9. Comparison of the variable and constant UA approaches for (a) the CH water inlet temperature, (b) the CH water outlet temperature, and (c) the DHW inlet and outlet temperature difference of the PHE at 5 l/min DHW request

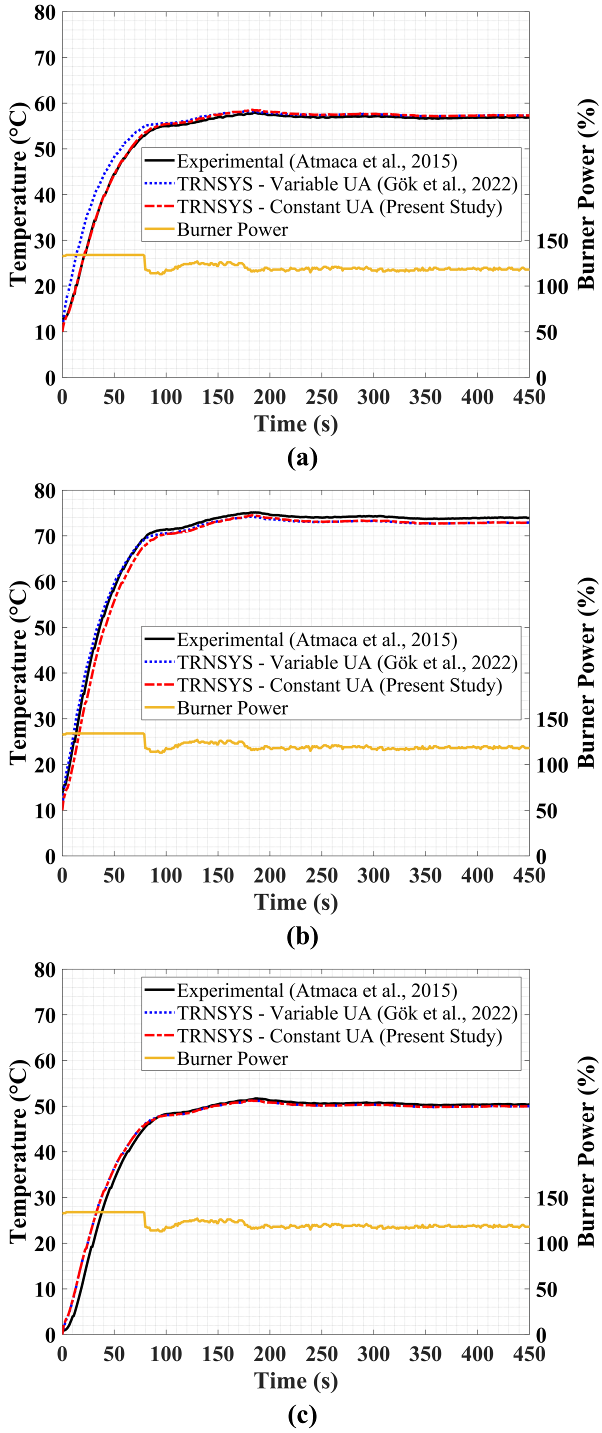

Figure 10. Display of the difference between the variable and constant UA approaches for (a) the CH water inlet temperature, (b) the CH water outlet temperature, and (c) the DHW inlet and outlet temperature difference at 7 l/min DHW user request

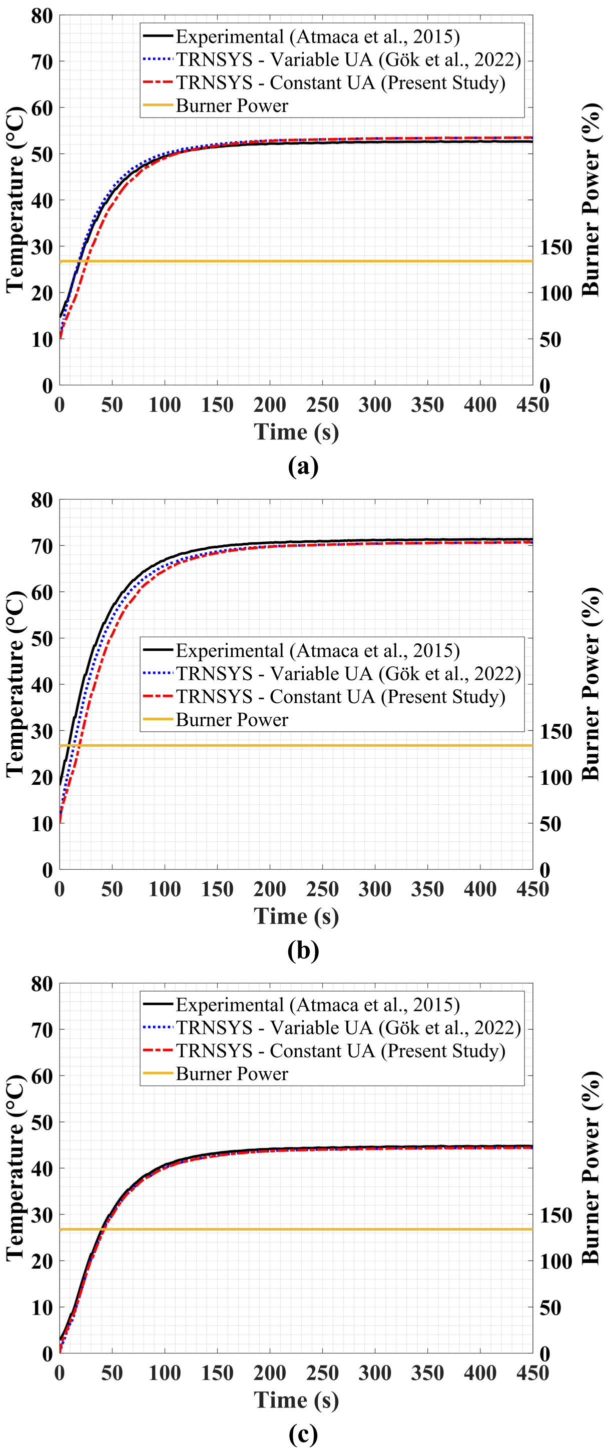

Figure 11. Comparative results of the variable and constant UA approaches for (a) the CH water inlet temperature, (b) the CH water outlet temperature, and (c) the DHW inlet and outlet temperature difference of the PHE at 8.7 l/min DHW request

The MAE values stay the same for the steady-state temperature profiles with respect to both of the approaches at the 8,7 l/min DHW user request simulation. CH water inlet temperature yields averagely 0,8°C error and CH water outlet temperature results in approximately 0,7°C for the same flow rate. Moreover, the MAE of the DHW inlet and outlet temperature difference is 0,4°C showing a good agreement between the modelling results and the experimental data. For the temperature profile covering the transient region as well, the MAE values for the CH inlet and outlet water increase, but they stay within an acceptable error range as given in Table 3. However, the temperature difference between the DHW inlet and outlet yields a good match with an approximate MAE value of 0.5 °C. To sum up all these discussions based on the constant and variable UA approaches, Table 2 is given for the error comparisons of the steady-state temperature profiles at various DHW flow rates and Table 3 displays the errors of the temperature profiles including the transient regions as well. In addition to MAE, the other metrics as MSE and RMSE are tabulated since they could be interpreted as in the same way of MAE.

Table 2. MAE, MSE, and RMSE comparisons between the variable and constant UA approaches with reference to steady-state region (between 200-500 seconds)

Error		5 l/min		7 l/min		8,7 l/min (eco mode)	
		Var. UA	Const. UA	Var. UA	Const. UA	Var. UA	Const. UA
$T_{CH,in}$	**MAE**	0.697	0.749	0.466	0.524	0.769	0.766
	MSE	0.490	0.569	0.220	0.281	0.594	0.591
	RMSE	0.700	0.755	0.469	0.530	0.770	0.769
$T_{CH,out}$	**MAE**	0.426	0.373	1.030	0.972	0.731	0.734
	MSE	0.184	0.150	1.064	0.955	0.536	0.542
	RMSE	0.428	0.387	1.032	0.977	0.732	0.736
ΔT_{DHW}	**MAE**	0.403	0.405	0.435	0.435	0.372	0.377
	MSE	0.164	0.166	0.193	0.191	0.139	0.143
	RMSE	0.405	0.407	0.439	0.437	0.373	0.378

Table 3. MAE, MSE, and RMSE comparisons between the variable and constant UA approaches including the transient and steady-state region (0-500 seconds)

Error		5 l/min		7 l/min		8,7 l/min (eco mode)	
		Var. UA	Const. UA	Var. UA	Const. UA	Var. UA	Const. UA
$T_{CH,in}$	**MAE**	0.928	1.224	1.215	0.492	0.774	1.051
	MSE	1.156	3.046	4.074	0.281	0.715	2.307
	RMSE	1.075	1.745	2.019	0.530	0.846	1.519
$T_{CH,out}$	**MAE**	0.771	1.630	1.019	1.345	1.279	2.039
	MSE	1.543	11.722	1.246	2.609	2.982	10.178
	RMSE	1.242	3.424	1.116	1.615	1.727	3.190
ΔT_{DHW}	**MAE**	0.464	0.464	0.814	0.818	0.528	0.536
	MSE	0.249	0.250	1.840	1.853	0.366	0.355
	RMSE	0.499	0.500	1.356	1.361	0.605	0.596

Validation of the Comfort Mode Operation

All these discussions are made with respect to the eco mode simulations. Up to now, it could be stated that constant UA approach would be utilized achieving a good agreement with the experimental data. Hence, for the comfort mode model validation, constant UA approach could be used. The available data in the literature includes the experimental DHW inlet and outlet temperature difference accompanied by the 1D modelling results (Atmaca et al., 2015). Making use of these data, TRNSYS model is validated both numerically and experimentally under constant UA approach in the comfort mode. When the DHW user demand is created in comfort mode, the appliance cannot start ignition directly since there is hot CH water in the system already. This late ignition time could be caught from the power profile given in Figure 12 as well. During this late ignition time, the DHW is heated by the heat retention of the HC preventing excessive temperature increase of the DHW which is also an uncomfortable case for the users resulting in scalding.

Hence there are two important respects to be inserted into the model appropriately regarding the comfort mode simulations as the variation of the UA profile during the late ignition time and the variation of the load profile when the ignition starts. The upper peaks in Figure 12 are arisen from the heat retention effects although ignition does not start directly and the lower peaks are observed subsequently since the system starts cooling during the late ignition time. There is no load profile introduced into the model during the late ignition time since the HC is assumed to provide the CH water at 60°C of outlet temperature due to its stored heat at the time of preheat cycles exemplified in Figure 3. As of the UA profile, the same assumption for the CH water outlet temperature from the HC which is 60°C is used. Since the DHW inlet and outlet temperatures of the PHE are measured experimentally at 8,7 l/min DHW user request, the CH inlet temperature of the HC could be obtained with the CH water outlet temperature assumption. Hence, UA profile during the late ignition time could be calculated and inserted into the model to evaluate the transient profile of the DHW temperature difference between the inlet and outlet of the PHE. By the way, the UA profile after the late ignition time is inserted into the model as a constant value defined for the DHW user request of the same flow rate in eco mode since the applicability of the constant UA approach is shown in the previous section.

Definition of the CH water outlet temperature at 60°C during the late ignition time due to the stored heat at the time of preheat cycles is a reasonable assumption as exemplified in Figure 3. Moreover, the assumed CH outlet temperature of 60°C is also supported from the temperature limitations stated by the literature studies. The DHW temperature limit is 60°C in order to produce a mixed fluid with the cold tap water not exceeding 48°C. Although there is an upper limit to prevent scalding for the DHW temperature, there is another problem bringing a lower limit as the colonization of bacteria, *Legionella.* The temperature of the water in the system should be above 60°C in order to reduce the risk of the bacteria (Boait et al., 2012). That's why, UA profiles and load profiles of 8,7 l/min DHW user request are given separately for the eco and comfort modes in Figure 6 and Figure 7, respectively.

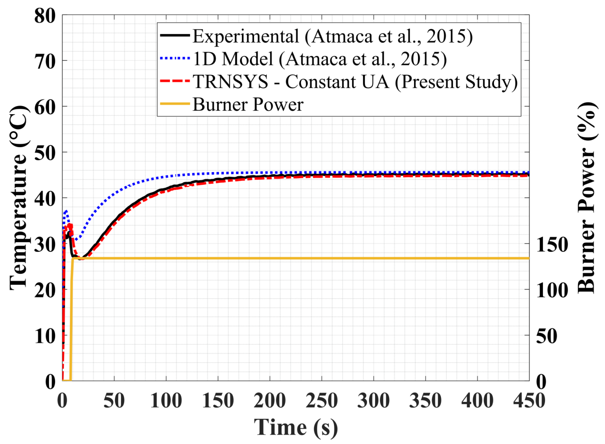

Figure 12. Validation of the comfort mode operation for 8.7 l/min user demand

After the late ignition time of 9 seconds, the appliance starts working and the power profile is recorded which is constant for the DHW user demand of 8,7 l/min. Heat transfer rate to the DHW is calculated from the flow rate of the DHW and DHW inlet and outlet temperature difference of the PHE. Hence the load profile after the late ignition time could be obtained in the comfort mode as the difference between the burner power and heat transfer rate of the DHW. The comfort mode load profile of 8,7 l/min DHW user request after the late ignition time has similar trend to the load profile of the same DHW flow rate in the eco mode, but the load profile of the comfort mode is smaller than that of the eco mode since the system components are still hot in the transient region.

In Figure 12, 1D modelling comfort mode calculations of Atmaca et al. (2015) as well are displayed in addition to the experimental data. For the steady-state region MAE values of the TRNSYS are decreased when compared to that of the 1D model. Generally speaking, the predictions of the both models yield a good agreement with the experimental data for the steady-state region. The greatest achievement of the model is the decrease of MAE value from 1.7°C of 1D model to 0.5°C of TRNSYS model for the temperature profile covering the transient region as well. As it is seen also from Figure 12, TRNSYS model predicts the lower and upper peaks of the DHW inlet and outlet temperature difference profile with a considerably small error when compared to the results obtained from the 1D model. The estimations regarding these peaks are of vital importance to the Waiting Time Test of the combi boiler comfort tests declared by the standards (BS EN 13203-1:2006, 2006). The reason for the better agreement of the TRNSYS modelling results is the experimental load profile inserted into the HC model in comparison with the 1D model. With the extension of a such model with various load profiles covering various operating conditions, a preliminary laboratory testing simulation tool could be proposed.

CONCLUSIONS

This study is a part of an ongoing research focusing on the DHW heating circuit models of the combi boilers. Previously 1D model has been established and validated experimentally. A commercial software has been used to model the DHW heating circuit as well and the applicability of such kind of modelling tool has been discussed. It is concluded that 1D model needs improvement since the discrepancy between the calculated results and the experimental data is to be diminished in the transient region although the agreement of the numerical results with the experimental data is found satisfactory for the steady-state region. Lastly, a TRNSYS model has been constructed for the same DHW circuit with the implementation of the variable load profile of the HC and the variable UA profile of the PHE based on the experimental measurements for various operating conditions of eco working mode. The outcomes from the TRNSYS model are categorized into three sections. Firstly, experimental validation of the TRNSYS model has been made for the eco working mode simulations. Secondly, the TRNSYS model has been validated numerically as well by solving 1D modelling equations of the HC and the PHE. MEA, MSE, and RMSE values of the TRNSYS model and 1D model have been compared with respect to the experimental data for all eco mode simulations. It has been apparently proved that TRNSYS model improves the error values especially for the transient region due to the insertion of the experimental UA variation and the load profiles.

In this study, the main objective is to improve the TRNSYS model decreasing its dependency on the experimental data. Therefore, the UA parameter definition of the PHE is investigated. Unlike the aforementioned TRNSYS model, this modified model uses constant UA approach instead of the variable UA profile. All results obtained under the variable UA approach are compared with the results of the constant UA assumption. The MAE values of the DHW inlet and outlet temperature difference, which is the most critical output of the model, are nearly the same under variable and constant UA approaches with respect to the experimental data for both steady-state temperature distribution and the overall temperature profile covering the transient region as well. MAE values for the same temperature difference profile including the overall time region are 0.46°C, 0.82°C, and 0.53°C for 5 l/min, 7 l/min, and 8,7 l/min, respectively, for the eco mode simulations under both of the UA approaches. Some of the MAE values for the intermediate temperature values such as CH water inlet and outlet temperatures increase under constant UA approach, but the error stays still within the acceptable error range. As a result, it is concluded that the constant UA approach could be used in the parameter definition of the PHE thereby decreasing the reliance of the TRNSYS model on the experimental data. For some of the simulations to test new designs, it is customary to have limited experimental data. Hence, the applicability of the model could be increased while decreasing the dependence of the parameter definitions on the experimental data. Actually, the selection of these approaches as constant or variable is a critical determination for some the TRNSYS components affecting the final outcomes, i.e. Type 140 – Constant UA and Type 141 – Varying UA.

Lastly, making use of the constant UA approach, the comfort mode validation is completed. The results of DHW inlet and outlet temperature difference obtained from TRNSYS and the previously established 1D model are compared as well with respect to experimental data. The upper and lower peaks in the transient DHW inlet and outlet temperature difference profile of the comfort mode are estimated better with the TRNSYS model. The superiority of the TRNSYS model is more obvious when the MAE values are compared with that of 1D model in the comfort mode validation. MAE value calculated for the DHW inlet and outlet temperature difference in comfort mode operating scheme decreases from 1.7 °C to 0.5 °C with the TRNSYS model. Definition of the UA profile during the late ignition time is made based on the heat retention of the HC. The better agreement of the TRNSYS model with the experimental data is due to the experimental parameter definition. With the implementation of the constant UA approach in the PHE, the reliance of the model on the experimental data is decreased, but the load profile is still inserted to the model to take the transient effects into account. To sum up, the TRNSYS model could be used for the performance estimations of the DHW circuit in both eco and comfort simulations. Therefore, the number of the testing could be decreased with the preliminary evaluations interpreted from the simulation results. As of the future targets, the load profiles could be inserted into the model for various operating conditions or it could be modelled and inserted into the model by a mathematical expression for the wide use of the DHW circuit TRNSYS models.

ACKNOWLEDGEMENT

The authors would like to convey their special thanks to Bosch Termoteknik Isıtma ve Klima San. Tic. A.Ş. for their valuable technical support and knowledge sharing.

NOMENCLATURE

ρ	Density, kg/m^3
c_p	Specific heat, J/kg·K
T	Temperature, ˚C
$\dot{m}$	Mass flow rate, kg/s
A_s	Heat transfer surface area, m^2
A_c	Flow cross-sectional area, m^2
A_o	Outer heat transfer surface area, m^2
A_{PHE}	Heat transfer area of each plate, m^2
h	Convective heat transfer coefficient, W/m^2·K
U	Overall heat transfer coefficient, W/m^2·K
l_{PHE}	Length of the PHE, m
s	HC height, m
t	Time, s
z	CH water flow length around the HC, m
k	Thermal conductivity, W/m·K

V_{chwc}	Volume of the CH water at each hot water channel of the PHE, m^3
V_{dhwc}	Volume of the DHW at each cold-water channel of the PHE, m^3
dx_1	Control volume length in x_1 direction, m
dx_2	Control volume length in x_2 direction, m
dy_1	Control volume height in y_1 direction, m
dy_2	Control volume height in y_2 direction, m
Q_{CH}	Amount of heat transferred from CH water to DHW, kJ
T_{adia}	Adiabatic flame temperature, ˚C
P	The appliance power at the steady-state operating region (without power modulation)
φ	Coefficient corresponding to the power modulation
P_{rated}	Rated power of the pump, kW
$\dot{V}$	Volume flow rate, l/min
$\dot{Q}$	Rate of heat transfer, kW
n	Total number of the measurements or calculations from a specified point
UA	Multiplication of the overall heat transfer coefficient and the heat transfer area, W/K
y	Measured or calculated parameter, i.e. temperature

Subscripts

g	Hot combustion gases
wt (1)	CH water in the HC
wt (2)	CH water in the PHE
wt (3)	DHW in the PHE
w	HC wall
wt	Water
∞	Surrounding air
comb	Combustion
pipe	Pipe in the CH circuit
in	Inlet
out	Outlet
load	Heat retention effect of the heat cell block in the CH water circuit (load definition)
initial	Initial value at simulation start
final	Final value at the simulation stop
rated	Nominal value
net	Net amount
exp	Experimental
theo	Theoretical
i	i^{th} number of the measurement or calculation
pump	Pump in the CH circuit

Abbreviations

CH	Central heating
DHW	Domestic hot water
DCW	Domestic cold water
PHE	Plate heat exchanger
HC	Heat cell
CV	Control volume
MAE	Mean absolute error
MSE	Mean square error
RMSE	Root mean square error

REFERENCES

Andrés A. C. and López J. M. C., 2002, TRNSYS model of a thermosiphon solar domestic water heater with a horizontal store and mantle heat exchanger, *Solar Energy*, 72(2), 89-98.

Antoniadis C. N. and Martinopoulos G., 2019, Optimization of a building integrated solar thermal system with seasonal storage using TRNSYS, *Renewable Energy*, 137, 56-66.

Atmaca A. U., Erek A., and Altay H. M., 2015, Investigation of Transient Behaviour of Combi Boiler Type Appliances for Domestic Hot Water, *Applied Thermal Engineering*, 82, 129-140.

Atmaca A. U., Erek, A., and Altay, H. M., 2016, Comparison of Two Numerical Approaches to the Domestic Hot Water Circuit in a Combi Boiler Appliance, *Energy and Buildings*, 127, 1043–1056.

Boait P. J., Dixon D., Fan D., and Stafford A., 2012, Production efficiency of hot water for domestic use, *Energy and Buildings*, 54, 160–168.

Bourke G. and Bansal P., 2012, New test method for gas boosters with domestic solar water heaters, *Solar Energy*, 86 (1), 78-86.

Braas H., Jordan U., Best I., Orozaliev J., and Vajen K., 2020, District heating load profiles for domestic hot water preparation with realistic simultaneity using DHWcalc and TRNSYS, *Energy*, 201, 117552.

BS EN 13203-1:2006, 2006, Gas-fired domestic appliances producing hot water- Appliances not exceeding 70 kW heat input and 300 l water storage capacity - Part 1: Assessment of performance of hot water deliveries.

Fridlyand A., Guada A. B., Kingston T., and Glanville P., 2021, Modeling modern, residential, combined space and water heating systems using EnergyPlus, *ASHRAE Transactions*, 127, 135-142.

Gök O., Atmaca A. U., Altay H. M., and Erek A., 2022, The Use of TRNSYS as a Simulation Tool for the Domestic Hot Water Performance Evaluations of the Combi Boilers, *Proceedings of the 2nd International Conference on Energy, Environment and Storage of Energy,* Kayseri, 96-97.

Gök O., Atmaca A. U., Altay H. M., and Erek A., 2023, Model of the Combi Boiler Appliance in TRNSYS for Domestic Hot Water Circuit: Experimental and Numerical Validations of Economic Mode Simulations, *International Journal of Energy Studies,* 8(1), 15-38.

Haissig C. M. and Woessner M., 2000, An adaptive fuzzy algorithm for domestic hot water temperature control of a combi-boiler, *HVAC&R Research*, 6:2, 117-134.

Harrabi I., Hamdi M., Bessifi A., and Hazami M., 2021, Dynamic modeling of solar thermal collectors for domestic hot water production using TRNSYS, *Euro-Mediterranean Journal for Environmental Integration*, 6:21.

Ibrahim O., Fardoun F., Younes R., and Louahlia-Gualous H., 2014, Review of water-heating systems: General selection approach based on energy and environmental aspects, *Building and Environment*, 72, 259-286.

Incropera F. P., Dewitt D. P., Bergman T. L., and Lavine A. S., 2007, *Fundamentals of heat and mass transfer* (6th ed.). USA: John Wiley & Sons, Inc.

Jordan U. and Vajen K., 2001, Influence of the DHW load profile on the fractional energy savings: A case study of a solar combi-system with TRNSYS simulations, *Solar Energy*, 69, 197-208.

Klein S. A. et al, 2017, TRNSYS 18: A Transient System Simulation Program, Solar Energy Laboratory, University of Wisconsin, Madison, USA, http://sel.me.wisc.edu/trnsys.

Lu M., Zhang C., Zhang D., Wang R., Zhou Z., Zhan C., Zai X., and Jing Q., 2021, Operational optimization of district heating system based on an integrated model in TRNSYS, *Energy & Buildings*, 230, 110538.

Nordlander S. G. and Persson T. G., 2003, Evaluation and computer modelling of wood pellet stoves with liquid heat exchanger, *ISES World Conference*, Gothenburg.

Pärisch P., Van der Veer N., Kirchner M., Giovannetti F., and Lampe C., 2019, Comfort assessment of tankless water heaters: Review and Suggestions, *IEA SHC International Conference on Solar Heating and Cooling for Buildings and Industry*.

Persson T., Fiedler F., Nordlander S., Bales C., and Paavilainen J., 2009, Validation of a dynamic model for wood pellet boilers and stoves, *Applied Energy*, 86(5), 645-656.

Persson T., Wiertzema H., Win K. M., and Bales C., 2019, Modelling of dynamics and stratification effects in pellet boilers, *Renewable Energy*, 134, 769-782.

Pomianowski M. Z., Johra H., Marszal-Pomianowska A., and Zhang C., 2020, Sustainable and energy-efficient domestic hot water systems: A review, *Renewable and Sustainable Energy Reviews*, 128, 109900.

Quintã A. F., Ferreira J. A. F., Ramos A., Martins N. A. D., and Costa V. A. F., 2019, Simulation models for tankless gas water heaters, *Applied Thermal Engineering*, 148, 944–952.

Shrivastava R. L., Kumar V., and Untawale S. P., 2017, Modeling and simulation of solar water heater: A TRNSYS perspective, *Renewable and Sustainable Energy Reviews*, 67, 126–143.

Ucar M. and Arslan O., 2021, Assessment of improvement potential of a condensed combi boiler via advanced exergy analysis, *Thermal Science and Engineering Progress*, 23.

Villa-Arrieta M. and Sumper A., 2018, A model for an economic evaluation of energy systems using TRNSYS, *Applied Energy*, 215, 765–777.